Computational investigation of quantitative entropy generation in centrifugal compressors with different exit beta angle

Dachdanai Boonchauy[1], Kittipass Wasinarom, Monthol Chamsab and Jaruwat Charoensuk[2]

Department of Mechanical Engineering, King Mongkut's Institute of Technology Ladkrabang,

Bangkok, Thailand 10520

* Corresponding Author: Tel: 0-2329-8351, Fax: 0-2329-8352,

E-mail: compdidCFD@gmail.com[1],kcjarruw@kmitl.ac.th[2]

Abstract

This research proposed for investigation on the quantitative entropy generation in the streamwise location of flow passage of centrifugal compressors with different exit beta angle which its operating condition designed for small gas turbine application. The flow field was obtained by 3D numerical simulation technique (CFD), with the help of commercial CFD code. The analysis was coupled both of flow structure and quantitative entropy that generation from the compressor inlet to the outlet. The comparison have been made between 10, 20, 30, 40 and 50 exit beta angle. The simulation result, shows the streamwise location of 0.1-0.6 entropy generate around 60 J/kg.K per streamwise location length for all exit beta angle, because of the inflow direction is parallel with the flow passage. In contrast, at the location 0.6-1.0 entropy generate around 480 J/kg.K per streamwise location length, around 8 times of the entropy generated in location 0.1-0.6. This is correspondent to the high deformation rate of the flow field in this area. The separation and secondary flow can be observed by blade tip leakage. Moreover, strong flow distortion resulting from switching the rotating reference frame to station reference frame, along with massive turbulent intensity that consequence in high local eddy viscosity. The beta angle was alleviated on jet-wake shear layer at the exit area of the compressor. Consequence in less entropy generation in such area.

Keywords: Entropy, flow passage, centrifugal compressor

1. Introduction

Small gas turbines engines become more practical means of power generation. Regarding to its many advantage comparing to piston engines. For examples, capability to operate with various fuel type, including low callorific fuel because of its continuous combustion process, more combustion efficiency, less emission. Although small gas turbine engine compression ratio was limited by turbine inlet temperature and components efficiency. Nowadays, compressor efficiency and

turbine inlet temperature with the help of CFD and material technology are increasing. Consequence in higher compression ratio and thermal efficiency of small gas turbine engine. Moreover, gas turbine exshuast gas temperature was typically much higher than piston engine. Consequence in higher potential to recover waste heat from exshaust gas. With heat recovery unit, it shows that small gas turbine engine can achieve thermal efficiency around 30%, which comparable to piston engine.

Electrical demands in remote area is normally less density than urban area, not allow hugh combine cycle power plant to be practical. In contrast, many small electrical generations plant that cover wide areas, and located near the raw material source that can be converted to bio-fuel are needed. Therefore, synthesis gas from agriculture materials is the interesting alternative choice.

Thermal efficiency of small gas turbine is strongly depend on its efficiency of 3 components which comprising of 1.) compressor 2.) combustion chamber 3.) turbine. In order to achieve high system thermal efficiency, Each components must operate with high efficiency at their operating condition. The operating condition of Individual component was obtained from thermodynamics analysis [16] which aiming to analyst for the system operating thermodynamics state to achieve the highest system thermal efficiency with the restriction of components efficiency and turbine material that able to withstand the firing temperature.

The Entropy generation is the parameter that quantitatively indicates on the energy transformation from useful pressure and kinetics form, to useless thermal energy that dissipated in fluid itself, or so called internal irreversibility. In compressor, the more dissipation means more input energy required to obtain the target exit pressure and flow rate of the compressor. The local entropy generation is depends on local internal flow field structure. The entropy generation in compressor and turbine are largely impact on system thermal efficiency [1]. The entropy generation is generally cast by isentropic efficiency. In order to design compressor that capable to operate with high isentropic efficiency at design condition. Designer must understand physical flow field that occur in the flow passage. The flow field characteristic is resulting from various interaction.

Despite two third of the entropy was generated in diffuser [2] but it has been studied that diffuser efficiency was largely dependent on impeller exit flow condition and the interaction at the transition area from impeller to diffuser inlet was significantly contribute to the overall compressor performance [3]. Flow in diffuser is beyond the scope of discussion in this paper.

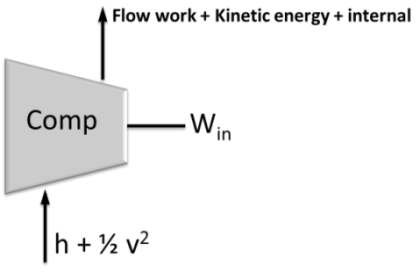

Fig 1. Compressor Energy analysis

One of the concern in changing any geometry parameter in order to improve efficiency of the centrifugal compressor is that the changing may shift the original operating condition. It has been investigated work that changing exit beta angle will contribute a little effect on Operating condition shifting [17].

2.1 Governing equations

3-D Reynolds averaged compressible Navier–Stokes equations was used for governing equations. The transport of momentum, mass, energy are taken into account. Eddy viscosity was computed by k–ε turbulent modeling. Mass and momentum transport equation can be written as below

$$\frac{\partial}{\partial x_i}\cdot\left(\rho u_i\right)=0 \tag{1}$$

$$\frac{\partial}{\partial x_j}\cdot\left(\rho u_i u_j\right)=-\frac{\partial P}{\partial x_i}+\frac{\partial}{\partial x_j}\left[\mu\left(\frac{\partial u_i}{\partial x_j}+\frac{\partial u_j}{\partial x_i}-\frac{2}{3}\delta_{ij}\frac{\partial u_l}{\partial x_l}\right)\right]$$
$$+\frac{\partial}{\partial x_j}\left[\mu\left(\frac{\partial u_i}{\partial x_j}+\frac{\partial u_j}{\partial x_i}\right)-\frac{2}{3}\left(\rho k+\mu_t\frac{\partial u_l}{\partial x_l}\right)\delta_{ij}\right] \tag{2}$$

The local entropy generation is depends on mean flow velocity gradient and level of turbulent intensity which can be computed via the equation below.

TKE transport and TKE dissipation transport can be computed using the transport equation as below

$$\frac{\partial}{\partial t}(\rho k)+\frac{\partial}{\partial x_i}(\rho k u_i)=\frac{\partial}{\partial x_j}\left[\left(\mu+\frac{\mu_t}{\sigma_k}\right)\frac{\partial k}{\partial x_j}\right]+P_k-\rho\varepsilon \tag{3}$$

$$\frac{\partial}{\partial t}(\rho\varepsilon)+\frac{\partial}{\partial x_i}(\rho\varepsilon u_i)=\frac{\partial}{\partial x_j}\left[\left(\mu+\frac{\mu_t}{\sigma_\varepsilon}\right)\frac{\partial\varepsilon}{\partial x_j}\right]+C_{\varepsilon 1}\frac{\varepsilon}{k}G_k-C_{\varepsilon 2}\rho\frac{\varepsilon^2}{k} \tag{4}$$

When σ_k and σ_ε are the turbulent prantl number which assigned to be constant equal to 1.0 and 1.3 respectively,

P_k is the local turbulent generation rate which is proportional to local mean flow velocity gradient, can be computed by the equation below

$$P_k=\left[\mu_t\left(\frac{\partial u_i}{\partial x_j}+\frac{\partial u_j}{\partial x_i}\right)-\frac{2}{3}\left(\rho k+3\mu_t\frac{\partial u_l}{\partial x_l}\right)\delta_{ij}\right]\frac{\partial u_j}{\partial x_i} \tag{5}$$

Turbulent viscosity (μ_t) can be calculated using k–ε turbulent modeling assumption as below which depends on local value of TKE and TKE dissipation rate

$$\mu_t=\rho C_\mu\frac{k^2}{\varepsilon} \tag{6}$$

When constant parameter $C_{\varepsilon 1}$, $C_{\varepsilon 2}$ and C_μ are assigned to be 1.44, 1.92 and 0.09 respectively.

3. Boundary conditions and numerical methodology

Preliminary compressor geometry was obtained corresponding to the designed thermodynamics cycle for 200 kW rated power gas turbines application [16]. The preliminary design procedure conducted on theoretical analysis basis that flow detail was not considered and many simplified assumptions were applied [4,5]. After that, CFD analysis was implement for flow analysis's detail and fine tuning of the flow passage were made in order to achieve high isentropic efficiency and desired operating condition.

Table 1 Thermodynamics analysis data

Isentropic Efficiency of Compressor	85%
Pressure Ratio	4
mass flow rate (kg/s)	1.33

Table 2 Geometry dimension from [9-11]

Dimension	Size
Inlet impeller diameter (mm)	90
Outlet impeller diameter (mm)	440
Inlet impeller height (mm)	15
Outlet impeller height (mm)	10
Number of impeller / splitter blade	9/9
Impeller speed (rpm)	20,000
Tip clearance (mm)[8]	1

3.1 Numerical methodology

The computational study has been conducted by commercial Ansys CFX Code [15] which was reputationed in turbo machinery flow modeling. The flow has been modeled with RANS scheme. k–ε Turbulent model was employed to predict turbulent property transport. Governing equation was discretized by Finite volume method. Flow domain was divided into 630,000 cells of structured hexahedral cell [6,8,14]. Grid independent was tested by compressor model of previous research [6,7] .The more grid density was executed in near wall region to capture more flow property gradient in that area. The normalized residual convergence criteria of every transport equation was set at 1.0e-04 [6][4][14]. Model validation was perform and good agreement outcome was achieved [6]. However, It need to be realized from the previous research in this area [13]. The different between steady and unsteady simulation was found.

It showed that the unsteady simulation gave more accurate result than the steady one. And it has revealed that the steady simulation (RANS) tends to predicted less entropy generation than the experiment and unsteady (URANS) simulation [12-14]. However, this has to be trade off with computer resource and more modeling complexity need to be concern.

3.2 Boundary Conditions and validations

- Inlet boundary condition, Static frame total pressure was assigned to 1 atm
- Outlet boundary condition, Average Static Pressure was assigned to 4 atm
- Stationary Wall and No-Slip Condition was assigned to wall
- Inlet temperature was 30 °C

The flow was modeled in steady flow regime. Air property was treated as compressible flow.

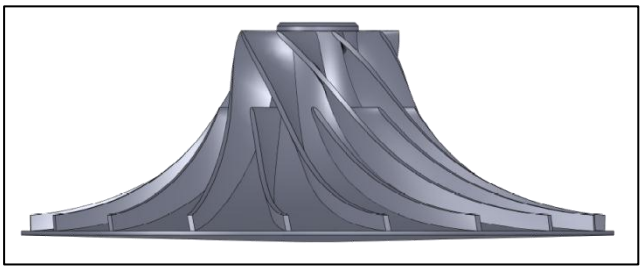

Fig 2. compressor geometry

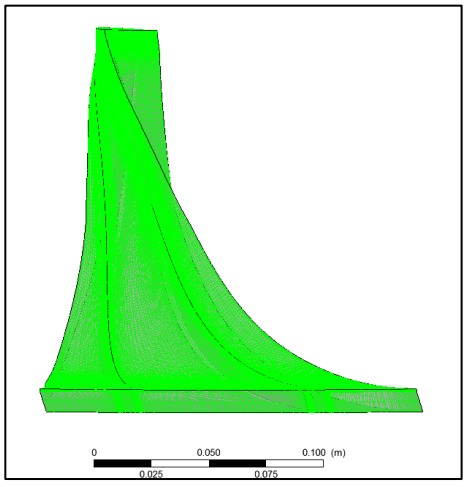

Fig 3. structure hexahedral mesh

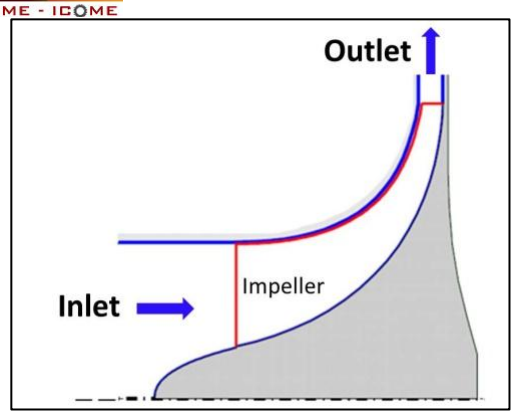

Fig 4. meridional plane of the computational domain

Model validation has been done by comparing the simulation result from Rigi Test Rig at Turbomachinery Laboratory.ETH Zurich [6,7] where the impeller model A8C41(Albert Kammerer) was employed. Good agreement between testing result and simulation result was obtained.

4. Results and Discussion

4.1 Quantitative entropy generation

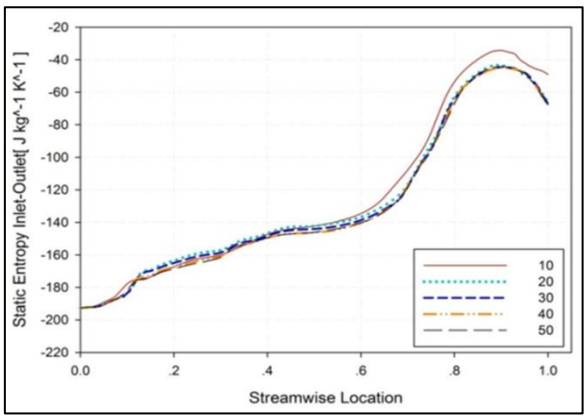

Fig 5. Static entropy at different stream-wise location for all exit beta angle

Regarding to the Figure 5. The simulation result shows the same character of entropy generation for all Beta(β_2) angle, at the stream-wise location range 0-0.6, the entropy generation was nearly linear characteristic, around 60 J/kg.K. But at the area just before the impeller exit, stream-wise location range 0.6-1.0 the entropy generation was around 8 times more than the impeller inlet region which around 480 J/Kg.K. Moreover, the highest entropy generation was found at the impeller exit region, in the case exit beta angle of 10 degrees and the lowest entropy generation was found in the case exit beta angle of 50 degrees.

4.2 The influence of exit beta angle on secondary flow region

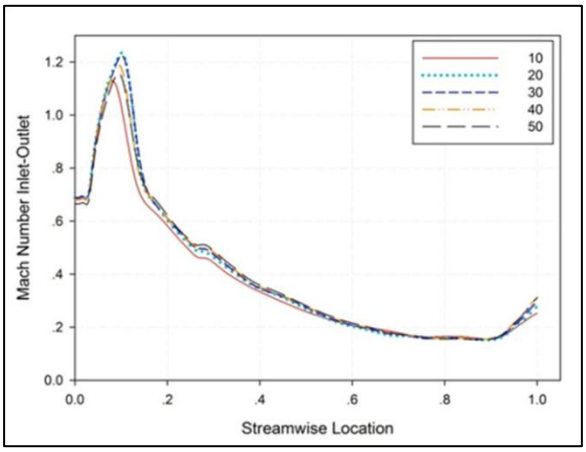

Fig 6. Mach number at various stream wise location for all exit beta angle

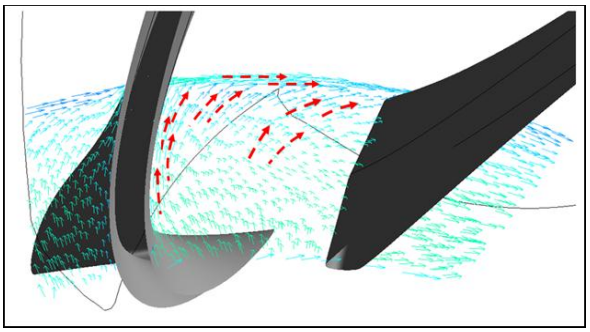

Fig 7. Secondary flow at stream-wise location of 0.25

At stream-wise location range of 0-0.6, flow stream line was paralleled with the flow

passage (Fig. 10 and 11) because the in-flow angle was same as the angle of the inlet impeller passage and the flow channel cross area was throated causing the fluid to accelerate along the flow passage in this range (Fig 6). It is easy to manage the flow in throat region since the flow momentum is become higher along the passage, so flow separation is more difficult to occur in throat region. However, this trade off with the flow blockage in throat region which limit allow mass flow rate of the compressor. Despite, there are no separation could be observed in the impeller inlet area, the secondary flow was formed from blade tip leakage flow that interaction with flow in the passage (Fig 7.)

In contrast with the Impeller inlet area (0.1-0.6 stream wise), the outlet area (0.6-1.0 stream wise) was difficulted to manipulate the flow since the flow was decelerated rapidly due to the wider area passage so called “diffuse”. Various physical interaction was effected on flow character in this area. In generally, Jet-wake region was found (Fig. 12 and 13). The low pressure and low velocity zone in the back side of the impeller blade was the cause of the flow separation since this region tend to suck the flow to separate from jet region. At the impeller outlet, jet-wake flow structure was interacted with the non-rotation frame resulting in recirculation flow at the impeller outlet (Fig 12 and 13). Stronger secondary flow from blade tip leakage interaction, comparing to the inlet region could be observed.

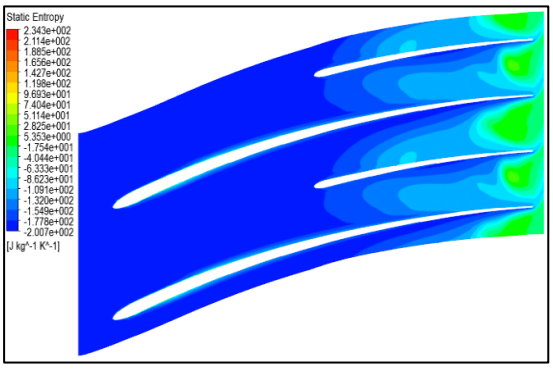

Fig 8. Entropy distribution of case 10 degree exit beta angle

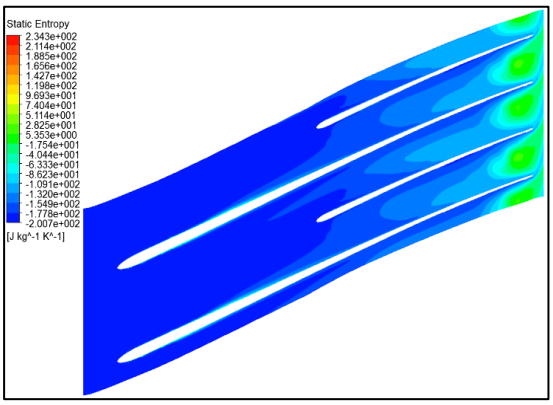

Fig 9. entropy distribution of case 50 degree exit beta angle

Fig. 8 and 9, shows entropy generation along stream-wise location of the impeller blade. It shows that at the location range of 0.1-0.6 entropy generation was very low, resulting from non-deformation flow field at the inlet area as stated before. At the location range of 0.1-0.6, the major source of entropy generation was came from near-wall region which shear layer comes from both secondary flow from blade leakage (Fig. 8 and 9) and boundary layer structure. At the location range of 0.5-0.7, found more entropy generation in near-wall region which coincide with the observed development on boundary layer and blade tip leakage interaction. However, entropy generation was in

the same level as the location 0-0.4 because the flow in this location was diffused, resulting in around 400% lower velocity magnitude (Fig 6). At the location of 0.7-1.0, entropy generation was 3-4 times of the location 0-0.6 because of the interaction of many physical interaction that leading to high deformation flow field. Starting from the separation flow in the region around 0.6 stream wise (Fig. 10 and 11) which was the commence of the two region or jet-wake flow structure, combine with the observed accumulated secondary flow along blade tip and accumulated turbulence intensity that generate from local high shear flow structure and convection from upstream flow.

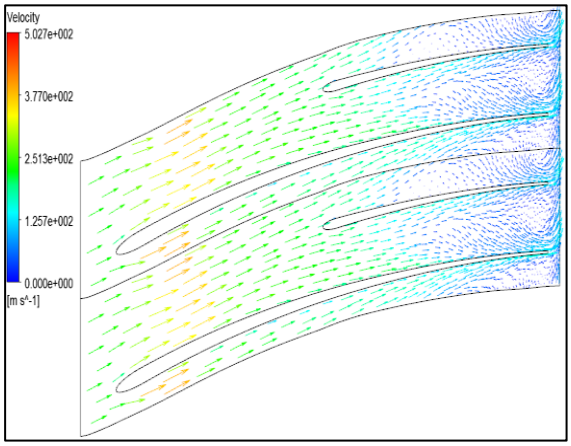

Fig. 10 velocity structure of 10 degree exit beta angle

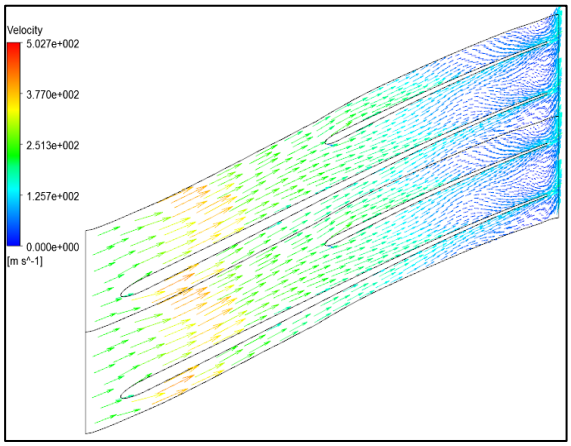

Fig. 11 velocity structure of 50 degree exit beta angle

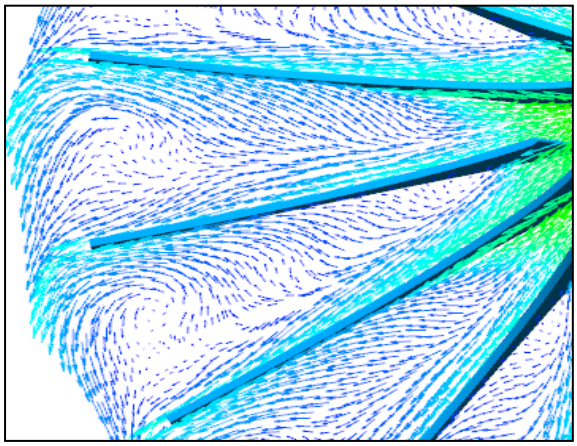

Fig. 12 Jet-wake and recirculation structure of 10 degree exit beta angle

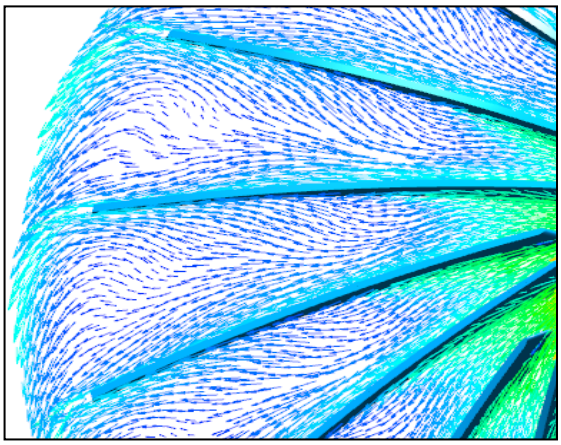

Fig. 13 Jet-wake and recirculation structure of 50 degree exit beta angle

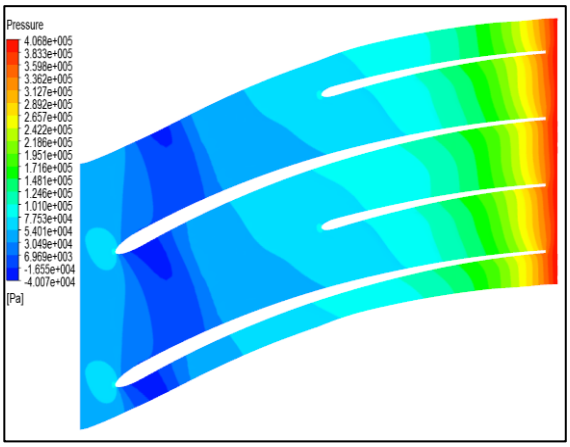

Fig. 14 pressure distribution of 10 degree exit beta angle

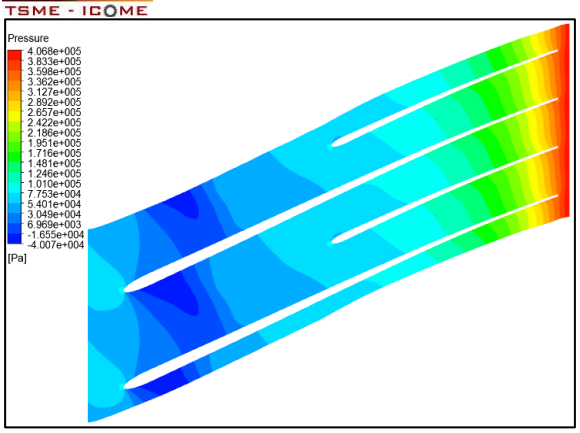

Fig. 15 pressure distribution of 50 degree exit beta angle

The beta angle was influenced on flow structure. The beta angle or back-swept angle was alleviated on the Jet-wake shear layer structure. Accelerate flow in wake region because Beta angle will resulting in smaller flow cross area (Fig 16) in wake region which cause the flow acceleration compare to smaller beta angle. In the other hand, Beta angle also influence in flow deceleration in jet region because of the wider area in the jet region Fig. 16

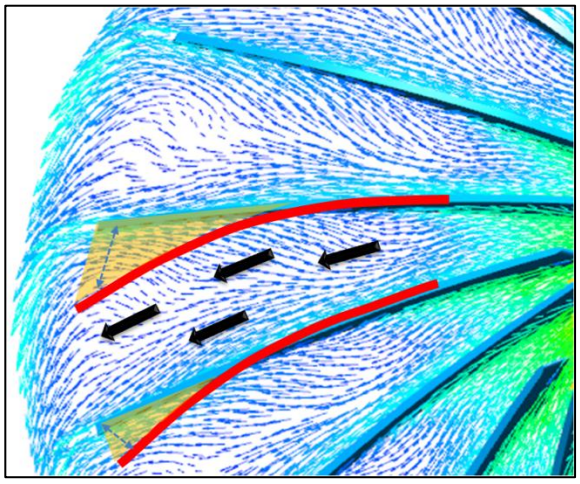

Fig. 16 effect of beta angle that cause smaller area in wake region and wider area in jet region

5. Conclusion

A computational investigation has been undertaken to investigate on the characteristic of entropy generation along blade passage of the centrifugal compressor, the effects of impeller exit beta angle on the entropy generation characteristic is also depict. Four different exit beta angle values are varied for this study. The following conclusions are derived from the computational analysis.

All four different exit beta angle are given the same entropy generation characteristic. At stream-wise location of 0.1-0.6 The entropy generation is almost the same for all four cases which is very little comparing to impeller exit region. At the impeller exit region (0.6-1.0 stream-wise) massive entropy generation occur. Because there are several physical interaction in this area.

The exit beta angle is effects on the impeller outlet flow pattern. Resulting in less entropy generated. The lowest entropy generation is observed in the case of beta angle 50 degree. The highest entropy generation occur in the case of beta angle 10 degree. The flow field velocity shows that exit beta angle effect on the flow structure in exit area, alleviate on the jet-wake shear layer and also impeller exit flow distortion, with its changing in exit flow angle.

The separation flow was earlier found in the case of low Beta angle. Also higher deformation rate of flow structure can be observed in the case of low beta angle.

6. References

[1] Soares, C. (2007). *Microturbines Application for Distributed Energy System*. London: Elsevier.

[2] Anish, S. and Sitaram, N. (2009) Computational investigation of impeller–diffuser interaction in a centrifugal compressor with different types of diffusers, Proceedings of the Institution of Mechanical Engineers, Part A: *Journal of Power and Energy*. 223:167-178

[3] Liu, R. and Xu, Z. (2004) Numerical investigation of a high-speed centrifugal compressor with hub vane diffusers, Proceedings of the Institution of Mechanical Engineers, Part A: *Journal of Power and Energy*. 218(3):155-169.

[4] Wilson, D. G. (1984). *The Design of High-Efficiency Turbomachinery and Gas Turbines.* Cambridge, MA:The MIT Press.

[5] Asuaje, M., Bakir, F., Smaine, K., and Rey, R. (2004). Inverse design method for centrifugal impellers and comparison with numerical simulation tools. *International Journal of Computacional Fluid Dynamics.* 18(2):101–110.

[6] Armin, Z., Albert, K. and Abhari, R.S. (2010). Unsteady Computational Fluid Dynamics Investigation on Inlet Distortion in a Centrifugal Compressor. *Journal of Turbomachinery*. 132.

[7] Schleer, M. and Abhari, R.S. (2008). Clearance Effects on the Evolution of the Flow in the Vaneless Diffuser of a Centrifugal Compressor at Part Load Condition. *Journal of Turbomachinery*. 130

[8] Tang, J., Turunen-Saaresti, T. and Lorjola, J. (2008). Use of partially shround impeller in asmall centrifugal compressor. *Journal of Thermal Science*. 17: 21-27.

[9] Baskharone, E.A. (2006). *Principle of Turbomachinery in Air-Breathing Engines*, Cambridge University, New York, Cambridge University Press

[10] Dixon, S.L. (2005). *Fluid mechanics and thermodynanics of turbomachinery*, Liverpool, Butterworth-Heinemann.

[11] Florin, L., Trevino, J. and Sommer, S. (2007). Numerical Analysis of Blade Geometry Generation Techniques for Centrifugal Compressors. *International Journal of Rotating Machinery*

[12] Trébinjac, I., Kulisa, P., Bulot, N. and Rochuon, N. (2009). Effect of Unsteadiness on the Performance of a Transonic Centrifugal Compressor Stage. *Journal of Turbomachinery*. 131.

[13] Dickmann, H.P., Wimmel, T.S., Szwedowicz, J., Filsinger, D., and Roduner, C.H. (2006). Unsteady Flow in a Turbocharger Centrifugal Compressor : Three-Dimensional Computational Fluid Dynamics Simulation and Numerical and Experimental Analysis of Impeller Blade Vibration. *Journal of Turbomachinery*. 128:455-465.

[14] Pierandreiand, G. and Sciubba, E. (2010). *Numerical Simulation and Entropy Generation Maps of an Ultra-Micro-*

Turbogas Compressor Rotor. ECOS 2010, 14-17 June 2010, Lausanne CH.

[15] ANSYS CFX-Solver Theory Guide. ANSYS CFX Release 12.1, *ANSYS Europe Ltd*., 1996-2006.

[16] กิตติภาส วศินารมณ์ และจารุวัตร เจริญสุข (2553). *การออกแบบและวิเคราะห์สมรรถนะห้องเผาไหม้เครื่องยนต์กังหันก๊าซขนาดเล็ก(200 กิโลวัตต์),* การประชุมวิชาการเครือข่ายวิศวกรรมเครื่องกลแห่ง ประเทศไทยครั้งที่ 24, 20-22 ตุลาคม 2553 จังหวัด อุบลราชธานี.

[17] เดชดนัย บุญช่วย. 2554. *"การจำลองเชิงตัวเลขคอมเพรสเซอร์แบบแรงเหวี่ยงสำหรับเครื่องยนต์กังหันก๊าซขนาดเล็ก (200 กิโลวัตต์)."* วิทยานิพนธ์ปริญญาวิศวกรรมศาสตรมหาบัณฑิต สาขาวิชาวิศวกรรมเครื่องกล บัณฑิตวิทยาลัย, สถาบันเทคโนโลยีพระจอมเกล้าเจ้าคุณทหารลาดกระบัง.